RCEPD With Enhanced Light Absorption by Crown-Shaped Quantum Well

Gun Wu Ju, Byung Hoon Na, Hee Ju Choi, Kwang Wook Park, Young Min Song, and Yong Tak Lee

***Abstract*— A high-performance resonant cavity enhanced photodetector (RCEPD) is developed by introducing an InGaAs/GaAs crown-shaped quantum well (CSQW) structure. In calculation, the absorption coefficient of the proposed CSQW structure is significantly enhanced by 47.8% compared with that of the conventional QW without increasing the electric field due to the large overlap of electron/hole-wave functions. To verify the feasibility of our proposed QW structure, we fabricate RCEPDs with a designed CSQW and the conventional QW structure. The fabricated CSQW-RCEPD exhibits a maximum quantum efficiency of 45.4%, an improvement of 36.2% in comparison with the conventional RCEPD. Moreover, the spectral bandwidth is 4.7 nm in the CSQW-RCEPD, which is in good agreement with the calculated result. The RCEPD with enhanced light absorption using a CSQW structure is highly promising for optical interconnect and sensing applications.**

***Index Terms*— Quantum well (QW), resonant-cavity-enhanced photodetector (RCEPD).**

I. Introduction

HIGH-SPEED photodetectors are key components which deliver a variety of high-throughputs in short reach optical interconnect systems such as board-to-board, module-to-module, and chip-to-chip interconnects [1]. However, there is a trade-off between speed and quantum efficiency (QE) in conventional p-i-n photodiodes due to the transit time, which in turn depends on the absorption thickness of the photodiode [2]. In order to solve this problem, thin absorption layers are inserted into a resonant cavity sandwiched by two mirrors. These resonant cavity enhanced photodetectors (RCEPDs) are based on the enhancement of the optical field in a Fabry-Perot (FP) cavity, and offer the possibility of overcoming the low QE limitation of conventional p-i-n photodiodes [3]. High reliability and high performance RCEPDs are crucial for optical interconnect [4]–[6] and optical sensing applications [7], [8].

The RCEPD structure can improve QE by increasing the reflectivity of the mirror. In previous reports, the RCEPD device had a narrow spectral bandwidth of light absorption due to the high quality factor of the FP cavity [9], [10]. The narrow spectral bandwidth of the QE can cause a misalignment problem of the cavity-mode wavelengths between the laser and detector, since wavelength overlap degrades significantly as the emission wavelength is changed by thermal red-shift. A wider spectral bandwidth can be obtained for RCEPD by reducing the pair of top mirrors, however, this approach results in a decreasing QE.

To realize an RCEPD with broad spectral bandwidth without degrading QE, the high absorption efficiency of a quantum well (QW) is essential. The absorption coefficient of a QW, which is proportional to oscillator strength, is well known to increase with decreasing quantum well thickness [11]. However, there is limit to achieve high oscillator strength by decreasing QW thickness due to the localization of carriers out of the well [12]. Also, the narrow QW structure requires more operating voltage because of the blue shift of the exciton absorption peak. In previous works, coupled quantum well (CQW) structures have been studied for large absorption coefficient [13], [14], but these characteristics were maintained under small bias voltage. This is because the electron/hole-wavefunctions of the reported CQW structures escaped from the well under large applied electric field.

In this letter, we designed a crown-shaped quantum well (CSQW) structure with two sub-barriers. The optical property of the CSQW structure was calculated and compared with a conventional QW structure. To verify the feasibility of our proposed CSQW structure, we fabricate RCEPDs with a designed CSQW and conventional QW structure. The QE of the CSQW-RCEPD was improved by 36.2% in comparison with the conventional RCEPD. Thus, the RCEPD with enhanced light absorption using the CSQW structure is highly promising for optical interconnect and sensing applications. Moreover, this result suggests great potential in other light absorption devices.

II. Design and Device Fabrication

Figure 1 show the energy band diagrams and thicknesses of conventional QW, narrow QW (NQW), stepped QW (SQW),

Manuscript received May 11, 2015; revised June 16, 2015; accepted June 22, 2015. Date of publication June 25, 2015; date of current version August 31, 2015. This work was supported in part by the GIST Systems Biology Infrastructure Establishment Grant (2014) and in part by the National Research Foundation of Korea through the Korea Government within the Ministry of Science, ICT and Future Planning under Grant NRF-20110017606.

G. W. Ju is with the School of Information and Communications, Gwangju Institute of Science and Technology, Gwangju 500-712, Korea (e-mail: gwju@gist.ac.kr).

B. H. Na is with the Imaging Device Laboratory, Samsung Advanced Institute of Technology, Suwon 443-803, Korea (e-mail: bhoon.na@samsung.com).

H. J. Choi is with the Graduate Program of Photonics and Applied Physics, Gwangju Institute of Science and Technology, Gwangju 500-712, Korea (e-mail: heeju@gist.ac.kr).

K. W. Park and Y. T. Lee are with the School of Information and Communications, Gwangju Institute of Science and Technology, Gwangju 500-712, Korea, and also with the Advanced Photonics Research Institute, Gwangju Institute of Science and Technology, Gwangju 500-712, Korea (e-mail: opticist@gist.ac.kr; ytlee@gist.ac.kr).

Y. M. Song is with the Department of Electronics Engineering, Pusan National University, Busan 609-735, Korea (e-mail: ymsong81@gmail.com).

Color versions of one or more of the figures in this letter are available online at http://ieeexplore.ieee.org.

Digital Object Identifier 10.1109/LPT.2015.2450022

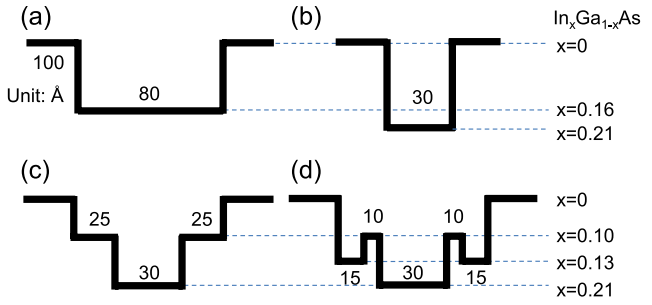

Fig. 1. Energy band diagrams and thicknesses of (a) conventional quantum well (QW), (b) narrow quantum well (NQW), (c) stepped quantum well (SQW), and (d) crown-shaped quantum well (CSQW) structures.

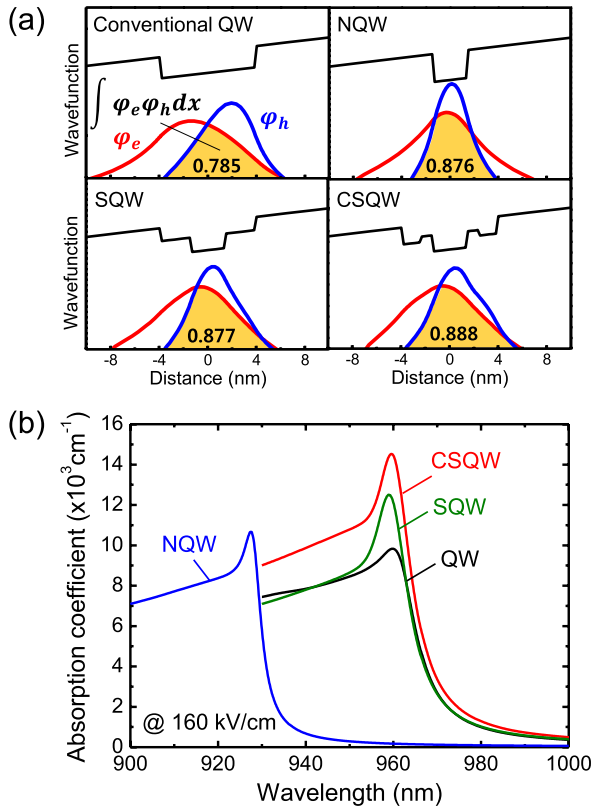

Fig. 2. (a) The electron/hole-wavefunctions with conduction band and (b) the calculated absorption coefficients of conventional QW, NQW, SQW, and CSQW structures under 160 kV/cm.

and proposed CSQW structures. The conventional QW structure consists of 80 Å-thick $In_{0.16}Ga_{0.84}As$ and 100 Å-thick GaAs barrier. To realize the large overlap of electron/hole-wavefunctions, we designed the NQW with a 30 Å-thick $In_{0.21}Ga_{0.79}As$, SQW with a 30 Å-thick $In_{0.21}Ga_{0.79}As$ and two 25 Å-thick $In_{0.10}Ga_{0.90}As$ sub-barriers, and CSQW with a 30 Å-thick $In_{0.21}Ga_{0.79}As$ narrow center well and two 15 Å-thick $In_{0.13}Ga_{0.87}As$ side wells separated by two 10 Å-thick $In_{0.10}Ga_{0.90}As$ sub-barriers.

To discuss the enhancement of absorption coefficient, we have calculated the electron/hole-wavefunctions and absorption coefficients of QW structures as shown in Figure 2. The QW modeling was performed using commercial software (APSYS Crosslight Software Inc.). The peak absorption

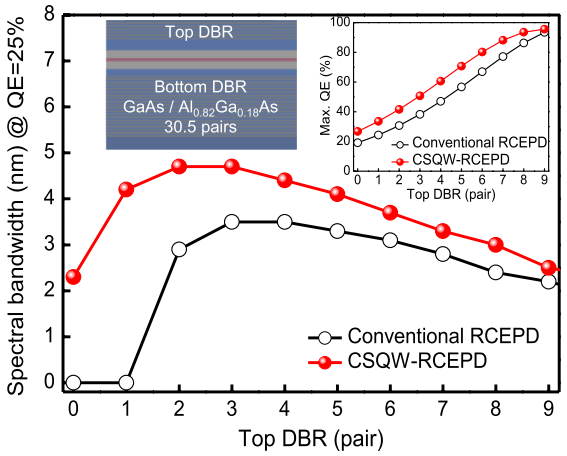

Fig. 3. The calculated spectral bandwidth at 25% QE as a function of top DBR pairs for conventional RCEPD and CSQW-RCEPD. The inset of Fig. 3 is schematic illustration of RCEPD and calculated maximum QE as a function of top DBR pairs.

coefficient of NQW structure is slightly higher than the one of conventional QW structure due to large overlap of electron/hole-wavefunctions. However, it is noteworthy that the absorption peak wavelength of the NQW structure is shorter than the one of conventional QW structure. Thus, it is hard to compare the NQW structure with other QW structures. It is true that we could validate QW narrowing effect by increasing indium composition of $In_xGa_{1-x}As$ QW ($x > 0.21$) to obtain the peak absorption wavelength which is same as the one of other QW structures. However, 30 Å-thick $In_xGa_{1-x}As$ QW having $x > 0.21$ is far beyond critical layer thickness, thus the QW is not a strained one anymore but a relaxed one. Due to the above mentioned physical limitation, we have designed the QW structure having narrow QW to obtain long absorption wavelength and high electron/hole wavefunctions overlap, coincidently. The SQW structure confines the carriers effectively in the QW region than the one of conventional QW structure. However, the carrier confined more effectively with the help of the CSQW structure increasing absorption coefficient. This is due to larger barrier height of the QW placed at the left side of the CSQW structure. The CSQW structure having the higher barrier restricts the tunneling of electron. Furthermore, the wavefunction of hole is also enhanced due to the QW placed at the right side of the CSQW structure. The absorption in the CSQW structure is enhanced by 47.8% in comparison with the conventional QW structure near the peak wavelength without increasing the electric field. Thus, the enhancement of absorption coefficient is a clear result of the CSQW structure having high barrier, narrow wells and coupling of the wavefunctions therein.

To demonstrate the concepts of our QW structure, we designed, fabricated, and characterized the RCEPD with CSQW (CSQW-RCEPD) and conventional RCEPD. The optical design of the RCEPDs were accomplished by using the transfer matrix method (TMM) based theoretical simulation. Figure 3 shows the calculated spectral bandwidth as a function of the top DBR pairs for CSQW-RCEPD and conventional RCEPD. As the top mirror reflectance increases, the calculated

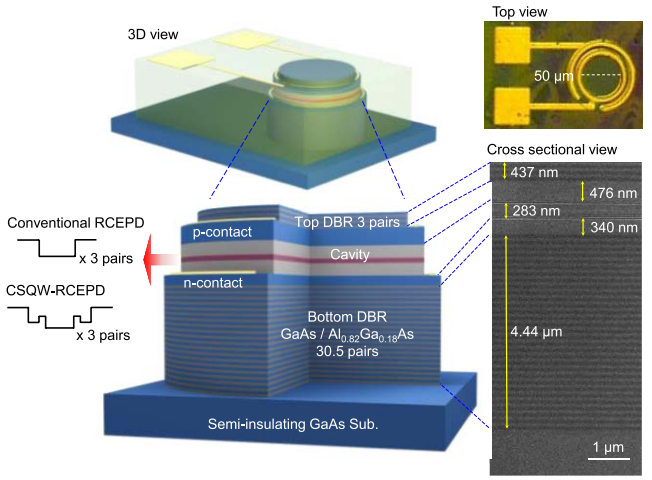

Fig. 4. 3D schematic illustration, top view microscope image and cross sectional scanning electron microscope image of the fabricated RCEPDs.

QE increases, but the spectral bandwidth decreases beyond 3 pairs of top DBR. Since the absorption coefficient of the CSQW structure was larger than the one of conventional QW structure, the CSQW-RCEPD showed enhanced QE and spectral bandwidth. In the case of wavelength division multiplexing, it should be noted that the light absorption range of the RCEPD is overlapped with the emission wavelength of the laser as a result of the misalignment problem caused by thermal red-shift. Therefore, the broad spectral bandwidth of QE can improve the manufacturing tolerance of sensing. Thus, the optimum number (3 pairs) was chosen to achieve a broadened spectral bandwidth with high QE.

Figure 4 shows a 3-dimensional (3D) schematic illustration, top view microscope image and cross sectional scanning electron microscope (SEM) image of the fabricated RCEPDs. All epitaxial layers were grown on semi-insulating (100) GaAs substrates by molecular beam epitaxy (DCA P600). To compare the electrical and optical performances, two RCEPD structures were grown which have different active regions; one is a CSQW structure, and the other is a conventional QW structure. The active regions surrounded by $Al_{0.3}Ga_{0.7}As$ cladding layers to form a 1 λ-thick cavity. This cavity was bounded on each side by n- and p-doped $5\lambda/4$-thick and $7\lambda/4$-thick GaAs contact layers, respectively. The top and bottom DBR mirrors without doping consisted of 3 and 30.5 pairs of $\lambda/4$-thick GaAs/$Al_{0.82}Ga_{0.18}As$ layers, respectively. For fabrication of RCEPDs, the samples were processed into a first cylindrical mesa of 50 μm in diameter etched down to the p-GaAs contact layer using an inductively coupled plasma etcher with an in situ laser interferometer [15]. Then, the second cylindrical mesa of 70 μm in diameter was etched down to the n-GaAs contact layer. The n-contact layer was etched for device isolation, and benzocyclobutene (BCB) was coated on the sample and cured at 210 °C for 1 hour for passivation and planarization. After exposing the p- and n-GaAs contact layers, Pt/Ti/Pt/Au and Ni/Au/Ge/Ni/Au metals were deposited on the p- and n-GaAs contact layers, respectively, using an electron-beam evaporator. The metal contacts were alloyed at 425 °C for 25 s.

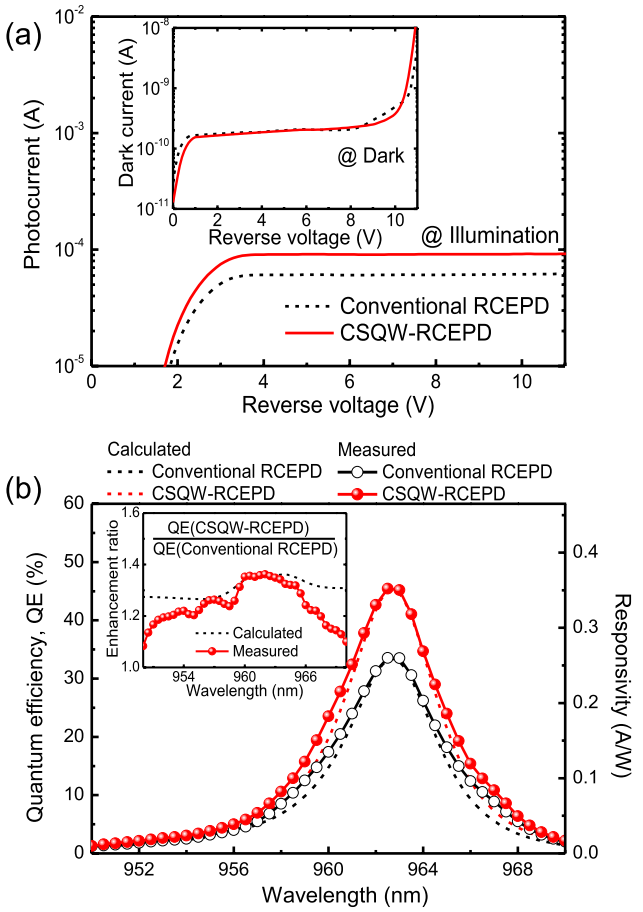

Fig. 5. (a) The measured dark and photocurrent as a function of reverse voltage and (b) calculated and measured QE of conventional RCEPD and CSQW-RCEPD. The inset of (b) shows the enhancement ratio of QE.

III. Result and Discussion

The performances of fabricated RCEPDs were measured by an experimental setup that consists of an external-cavity tunable laser source, a semiconductor parameter analyzer, an optical spectrum analyzer, and a standard optical powermeter. The dark current and photocurrent were measured as a function of reverse voltage as shown Figure 5(a). The photocurrent was measured under illumination with 962.5 nm lasing wavelength. The dark currents of conventional RCEPD and CSQW-RCEPD show similar as shown inset of Figure 5(a). However, the photocurrent of CSQW-RCEPD was higher than conventional RCEPD because of higher absorption characteristics.

The QE derived from responsivity which measured by photocurrent and input light power as a function of lasing wavelength. The measured spectral bandwidth of the conventional RCEPD and CSQW-RCEPD were 3.0 nm and 4.7 nm at QE = 25%, respectively, which was in good agreement with the calculated results, as shown in Figure 3. Moreover, the spectral bandwidth of the CSQW-RCEPD was broader than that of the conventional RCEPD structure because of the high and broad absorption coefficient in the CSQW.

The measured maximum QE values of the conventional RCEPD and CSQW-RCEPD were 33.5% and 45.4% at 962.5 nm, respectively. Unfortunately, the measured

QE values of RCEPDs were lower than that of the calculated values as shown in the inset of Figure 3. Due to errors in fabrication of the layer thickness growth, the measured peak wavelengths shift was longer than the designed wavelength. As the FP wavelength increased, the absorption coefficient shifted to long wavelength, and hence the intensity of absorption coefficient decreased because of decreasing overlap of electron/hole-wavefunctions. For the reasons mentioned above, we re-calculated the QE of the RCEPD by changing the thickness of the epitaxial layers and absorption coefficient under high bias voltage as shown in Figure 5 (b). As result, the measurement results of QE were well matched with re-calculated results.

In order to compare the QE between two RCEPDs, the enhancement ratio values are shown in the inset of Figure 5 (b). For the CSQW-RCEPD, the measured QE was enhanced by a factor of 1.362 as compared with the conventional RCEPD due to the high absorption of the CSQW structure. This enhancement result was slightly higher than the calculated value of 1.357. It seems quite probable that the CSQW structure maintained higher absorption than the conventional QW structure under large bias. This result makes it clear that the CSQW structure enhanced the light absorption in the optoelectronic device.

IV. Conclusion

In summary, we have numerically and experimentally demonstrated an enhanced light absorption RCEPD by substituting a CSQW structure for the conventional QW structure in an RCEPD and controlling the electron/hole-wavefunctions inside the well. A design with a maximum QE of 50.8% and a spectral bandwidth of 4.7 nm has been presented, fabricated, and characterized. Experimental results with a maximum QE of 45.4% and a spectral bandwidth of 4.7 nm were obtained. The mismatch of QE between the calculated design and the actual device was due to errors in fabrication of the layer thickness growth. Although the maximum QE value of CSQW-RCEPD was lower than the calculated design, it was enhanced by a factor of 1.362 as compared with the conventional RCEPD. Thus, it can be expected that the RCEPD with enhanced light absorption using a CSQW structure will be helpful for optical interconnect and sensing applications.

References

[1] A. F. Benner, M. Ignatowski, J. A. Kash, D. M. Kuchta, and M. B. Ritter, "Exploitation of optical interconnects in future server architectures," *IBM J. Res. Develop.*, vol. 49, nos. 4–5, pp. 755–775, Jul. 2005.

[2] A. Chin and T. Y. Chang, "Enhancement of quantum efficiency in thin photodiodes through absorptive resonance," *J. Lightw. Technol.*, vol. 9, no. 3, pp. 321–328, Mar. 1991.

[3] D. S. Golubović, P. S. Matavulj, and J. B. Radunović, "Characterization and optimization of a resonant cavity enhanced P-i-N photodiode response," *Int. J. Infr. Millim. Waves*, vol. 20, no. 1, pp. 109–123, Jan. 1999.

[4] S. Q. Luong *et al.*, "Monolithic wavelength-graded VCSEL and resonance-enhanced photodetector arrays for parallel optical interconnects," *IEEE Photon. Technol. Lett.*, vol. 10, no. 5, pp. 642–644, May 1998.

[5] Y. Zhou, J. Cheng, and A. A. Allerman, "High-speed wavelength-division multiplexing and demultiplexing using monolithic quasi-planar VCSEL and resonant photodetector arrays with strained InGaAs quantum wells," *IEEE Photon. Technol. Lett.*, vol. 12, no. 2, pp. 122–124, Feb. 2000.

[6] I.-S. Chung and Y. T. Lee, "A method to tune the cavity-mode wavelength of resonant cavity-enhanced photodetectors for bidirectional optical interconnects," *IEEE Photon. Technol. Lett.*, vol. 18, no. 1, pp. 46–48, Jan. 1, 2006.

[7] E. Thrush *et al.*, "Integrated semiconductor vertical-cavity surface-emitting lasers and PIN photodetectors for biomedical fluorescence sensing," *IEEE J. Quantum Electron.*, vol. 40, no. 5, pp. 491–498, May 2004.

[8] T. O'Sullivan *et al.*, "Implantable semiconductor biosensor for continuous in vivo sensing of far-red fluorescent molecules," *Opt. Exp.*, vol. 18, no. 12, pp. 12513–12525, Jun. 2010.

[9] I.-H. Tan *et al.*, "High quantum efficiency and narrow absorption bandwidth of the wafer-fused resonant $In_{0.53}Ga_{0.47}As$ photodetectors," *IEEE Photon. Technol. Lett.*, vol. 6, no. 7, pp. 811–813, Jul. 1994.

[10] M. S. Ünlü and S. Strite, "Resonant cavity enhanced photonic devices," *J. Appl. Phys.*, vol. 78, no. 2, pp. 607–639, Jul. 1995.

[11] S. Nojima and K. Wakita, "Optimization of quantum well materials and structures for excitonic electroabsorption effects," *Appl. Phys. Lett.*, vol. 53, no. 20, pp. 1958–1960, Mar. 1988.

[12] C. Monier, A. Freundlich, and M. F. Vilela, "Oscillator strength of excitons in (In, Ga)As/GaAs quantum wells in the presence of a large electric field," *J. Appl. Phys.*, vol. 85, no. 5, pp. 2713–2718, Mar. 1999.

[13] H. Feng, J. P. Pang, M. Sugiyama, K. Tada, and Y. Nakano, "Field-induced optical effect in a five-step asymmetric coupled quantum well with modified potential," *IEEE J. Quantum Electron.*, vol. 34, no. 7, pp. 1197–1208, Jul. 1998.

[14] N. Susa and T. Nakahara, "Enhancement of change in the absorption coefficient in an asymmetric quantum well," *Appl. Phys. Lett.*, vol. 60, no. 19, pp. 2324–2326, May 1992.

[15] Y. M. Song, K. S. Chang, B. H. Na, J. S. You, and Y. T. Lee, "Precise etch-depth control of microlens-integrated intracavity contacted vertical-cavity surface-emitting lasers by in-situ laser reflectometry and reflectivity modeling," *Thin Solid Films*, vol. 517, no. 19, pp. 5773–5778, Aug. 2009.